

MIT Open Access Articles

Redox Switchable Thianthrene Cavitands

The MIT Faculty has made this article openly available. **Please share** how this access benefits you. Your story matters.

Citation: Ong, Wen, et al. "Redox Switchable Thianthrene Cavitands." *Synthesis*, vol. 49, no. 02, Nov. 2016, pp. 358–64.

As Published: <http://dx.doi.org/10.1055/s-0036-1588659>

Publisher: Thieme Publishing Group

Persistent URL: <http://hdl.handle.net/1721.1/114719>

Version: Original manuscript: author's manuscript prior to formal peer review

Terms of use: Creative Commons Attribution-Noncommercial-Share Alike





Redox Switchable Thianthrene Cavitands

Journal:	SYNTHESIS
Manuscript ID	Draft
Manuscript Type:	Original Paper
Date Submitted by the Author:	n/a
Complete List of Authors:	Ong, Wen ; MIT, Chemistry Bertali, Federico; Universita degli Studi di Parma, Chemistry Dalcanale, Enrico; Universita degli Studi di Parma, Chemistry Swager, Timothy; MIT, Chemistry
Keywords:	calixarenes, supramolecular chemistry, redox active, physical organic, host-guest systems
Abstract:	A redox activated vase-to-kite conformational change is reported for a new resorcinarene-based cavitand appended with four quinoxaline-fused thianthrene units. In its neutral state, the thianthrene-containing cavitand was shown by ¹ H NMR to adopt a closed vase conformation. Upon oxidation the electrostatic repulsion among the thianthrene radical cations promotes a kite conformation in the thianthrene-containing cavitand. The addition of acid produced a shoulder feature below 300 nm in cavitand's UV-Vis spectrum that we have assigned to the vase-to-kite conformation change. UV-Vis spectroelectrochemical studies of the cavitand revealed a development of a similar shoulder peak consistent with the oxidation-induced vase-to-kite conformation change. To support that the shoulder peak is diagnostic for a vase-to-kite conformation change, a model molecule constituting a single quinoxaline wall of the cavitand was synthesized and studied. As expected UV-Vis spectroelectrochemical studies of the cavitand arm did not display a shoulder peak below 300 nm. The oxidation-induced vase-to-kite conformation is further confirmed by the distinctive upfield shift in ¹ H chemical shift of the methine signal.

SCHOLARONE™
Manuscripts

Redox Switchable Thianthrene Cavitanths

Wen Jie Ong^a
 Federico Bertani^{b,1}
 Enrico Dalcanele^b
 Timothy M. Swager^{a,*}

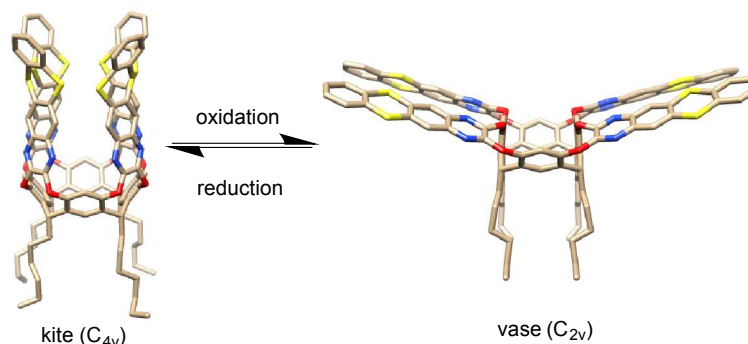
^a Department of Chemistry, Massachusetts Institute of Technology, 77 Massachusetts Avenue, Cambridge, Massachusetts 02139, United States

^b Department of Chemistry, University of Parma and INSTM RU, Parco Area delle Scienze 17/A, Parma 43124, Italy

* indicates the main/corresponding author.

tswager@mit.edu

[Click here to insert a dedication.](#)



Received:
 Accepted:
 Published online:
 DOI:

Abstract A redox activated vase-to-kite conformational change is reported for a new resorcinarene-based cavitaanth appended with four quinoxaline-fused thianthrene units. In its neutral state, the thianthrene-containing cavitaanth was shown by ¹H NMR to adopt a closed vase conformation. Upon oxidation the electrostatic repulsion among the thianthrene radical cations promotes a kite conformation in the thianthrene-containing cavitaanth. The addition of acid produced a shoulder feature below 300 nm in cavitaanth's UV-Vis spectrum that we have assigned to the vase-to-kite conformation change. UV-Vis spectroelectrochemical studies of the cavitaanth revealed a development of a similar shoulder peak consistent with the oxidation-induced vase-to-kite conformation change. To support that the shoulder peak is diagnostic for a vase-to-kite conformation change, a model molecule constituting a single quinoxaline wall of the cavitaanth was synthesized and studied. As expected UV-Vis spectroelectrochemical studies of the cavitaanth arm did not display a shoulder peak below 300 nm. The oxidation-induced vase-to-kite conformation is further confirmed by the distinctive upfield shift in ¹H chemical shift of the methine signal.

Key words redox active - thianthrene - resorcinarene cavitanths - electrochemical switching - conformation change

Since the first reported synthesis of quinoxaline-bridged resorcinarene cavitaanth by Cram and co-workers in 1982,² the diversity and complexity in both the structures and functionalities of cavitaanth derivatives have expanded dramatically. To date, cavitanths have found utility as switches,³ receptors,⁴ sensors,⁵ catalysts,⁶ molecular hosts,⁷ molecular grippers⁸ and solid-phase microextractors.⁹ Many of these applications hinge on the ability of quinoxaline-bridged cavitanths to adopt, often in response to an external stimulus, two spatially well-defined conformations: closed "vase" and open "kite" forms.

Resorcinarene cavitanths with four quinoxaline bridges are known to undergo vase-kite conformational switching induced by changes in temperature,¹⁰ pH,¹¹ and metal ion concentration.¹² To harness the unique conformational switching properties of these cavitanths in electronic devices, we have sought to effect the vase-kite conformation by redox reactions. In 2006, Diederich reported electrochemical molecular switching using a tetrathiafulvalene (TTF)-bridged resorcinarene cavitaanth.¹³ The incorporation of electroactive TTF groups in quinoxaline-based cavitanths is synthetically challenging and changes in the cyclic voltammetry and

differential pulse voltammetry spectra were used as evidence for electrochemically-induced vase-to-kite conformation change. More recently, the same group developed quinone-based, redox-active resorcinarene cavitanths that utilize intramolecular hydrogen bonding, which is only present in the reduced hydroquinone state, to stabilize the vase conformation.¹⁴ While such a system successfully demonstrated the viability of redox switchable cavitanths, the deployment of quinone-based cavitanths in electronic devices is limited by the need for an external proton source (e.g. a protic solvent). Moreover, electrochemical kinetics requiring coupled delivery of protons is often sluggish. To circumvent these problems, Peris and co-workers recently reported a tetraferrocenyl-resorcinarene cavitaanth as a redox-switchable host for ammonium salts.¹⁵ However, this cavitaanth remains in vase conformation in both the neutral and +4 oxidation states.

Hence, there is still a need for redox-active resorcinarene cavitanths that are readily synthesized and undergo rapid electrochemically-induced vase-kite conformation changes. Herein, we report the synthesis and conformational switching properties of a novel resorcinarene-based cavitaanth **1** featuring four quinoxaline-fused thianthrene units (Figure 1).

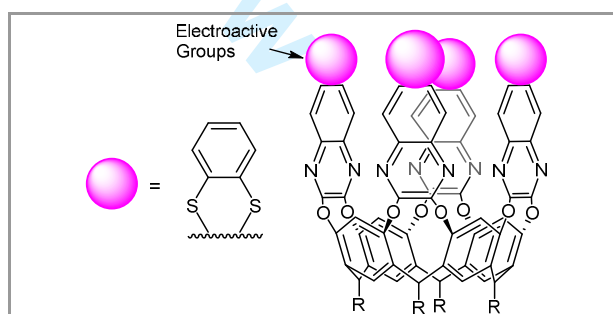


Figure 1 Structure of thianthrene-containing cavitaanth **1**

Thianthrene has been studied extensively for its redox activity,¹⁶ and a peculiar aspect of its redox chemistry is the geometric changes that accompany oxidation (Figure 2). In its neutral state, thianthrene is a bent molecule with a fold angle of 128° between the two planes of benzene rings. The folded structure appears to be favored in the neutral state to avoid repulsion between occupied 3p_z(Sulfur)-π*_{cc} orbitals.¹⁷ Upon oxidation, both

the radical cation and the dication are planar with a fold angle of $\sim 180^\circ$ (Figure 2).¹⁸ We hypothesized that neutral **1** will adopt the vase conformation and with oxidation electrostatic repulsion among the thianthrene radical cations will favor the kite conformation (Figure 3). The combination of the thianthrene and cavitand conformational changes has the prospect to endow these systems with new electroactive complexing properties.

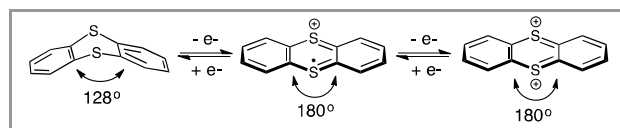


Figure 2 Different redox states of thianthrene and their corresponding fold angles

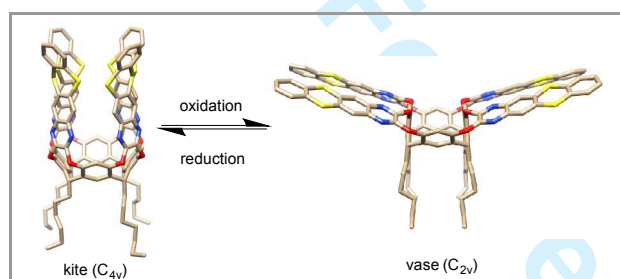


Figure 3 Vase-kite conformation change of thianthrene-containing cavitand **1** upon electrochemical stimuli

To demonstrate electrochemical switching, thianthrene-containing cavitand **1** was synthesized (Scheme 1). Dibromothianthrene **2** was synthesized from an S_NAr reaction between benzene-1,2-dithiol and 1,2-dibromo-4,5-difluorobenzene as previously reported.¹⁹ Using a modified procedure,²⁰ palladium-catalyzed Buchwald-Hartwig amination of **2** with benzophenone imine yielded diimine **3**, which upon acidic hydrolysis followed by basic work-up afforded diamine **4**. The condensation reaction of **4** with oxalic acid gave diol **5**, which was in turn subjected to thionyl chloride to give dichloride **6**, a key intermediate to this synthesis. Finally, cavitand **1** was obtained by S_NAr reaction of **6** with resorcinarene ($R = C_6H_{13}$). This six-step synthesis is accomplished in an overall yield of 28%.

For electrochemical actuation cavitand **1** should be: 1) in the vase conformation while in a neutral state at room temperature, and 2) convert to the kite conformation upon oxidation. Vase-to-kite conformation changes can be monitored by the distinctive methine chemical shift from *ca.* 5.5 ppm (vase conformation) to *ca.* 3.8 ppm (kite conformation),²¹ and by a change in the UV-Vis spectrum.¹¹ Therefore, we sought to validate the abovementioned two criteria using both 1H NMR and UV-Vis spectroscopy.

The methine signal for cavitand **1** in neutral state at room temperature was 5.20 ppm and hence, based on literature data, **1** is in vase conformation. Quinoxaline-based cavitands are known to undergo vase-to-kite conformation change upon protonation and at low temperatures. Hence, we treated **1** with trifluoroacetic acid (TFA) and also did variable temperature studies. With addition of TFA the thianthrene-containing cavitand **1** adopts the kite conformation, as evident from the 5.20 ppm methine signal (vase conformation) shifting to 3.90 ppm (kite conformation) (Figure 4). Similarly, we observe a gradual upfield shift in the methine proton resonance with decreasing temperature (see Supporting Information).

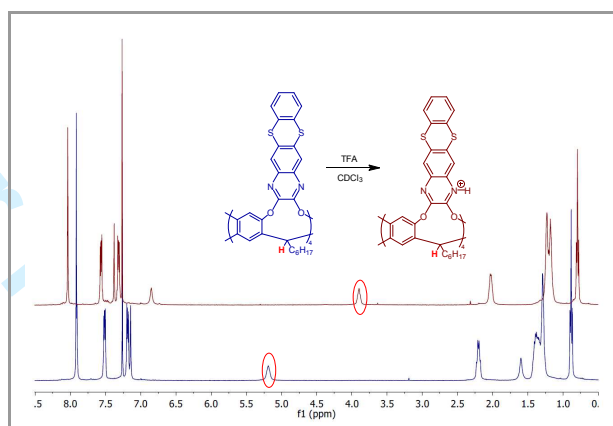
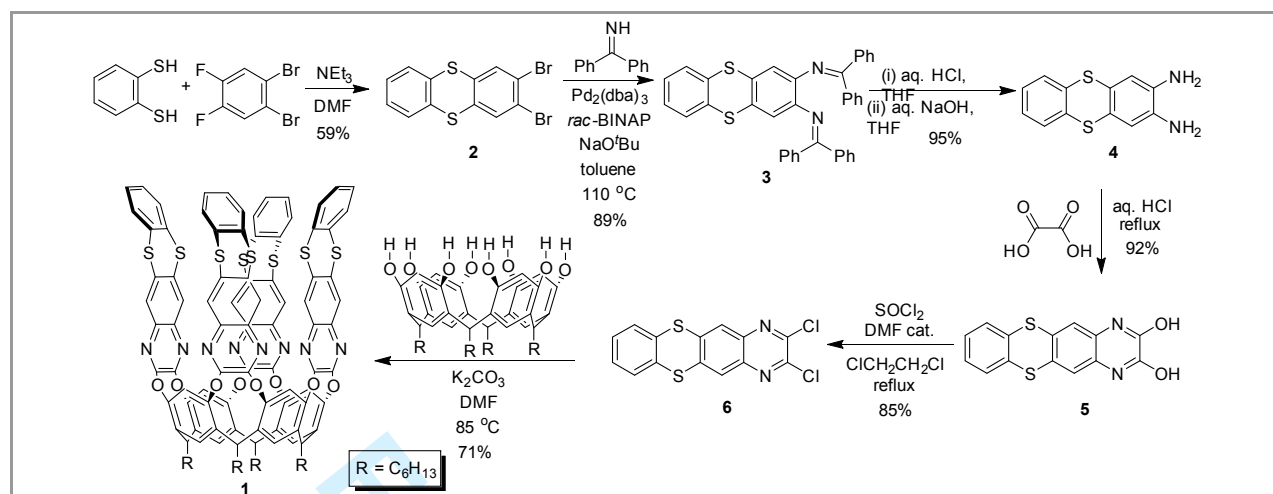
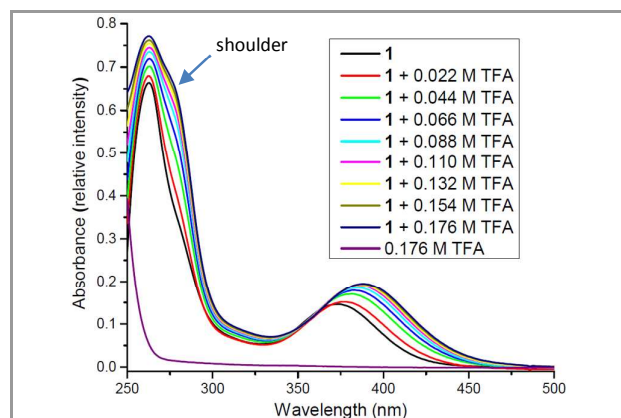
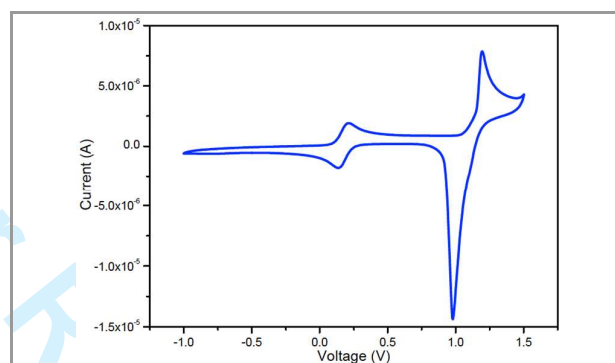
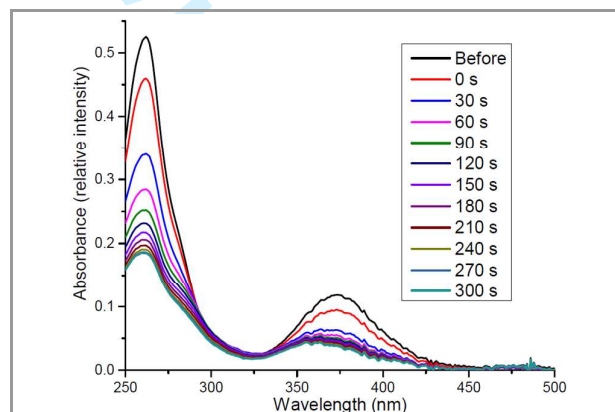


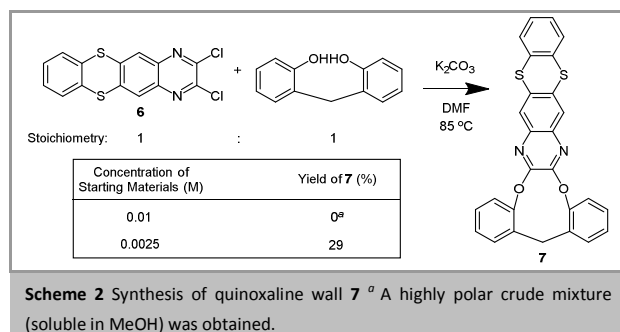
Figure 4 1H NMR spectra of **1** before (blue) and after (maroon) addition of TFA

Scheme 1 Synthesis of thianthrene-containing cavity **1**.

Treatment with TFA produced a shoulder peak below 300 nm in the UV-Vis spectra of **1** (Figure 5), which led us to hypothesize that the vase-to-kite conformation change is responsible for the development of this shoulder peak. Compound **1** can also be oxidized electrochemically (Figure 6) and UV-Vis spectroelectrochemical measurements conducted above the oxidation peak potential (Figure 7) revealed the development of a similar shoulder peak below 300 nm. Again this is consistent with **1** undergoing a vase-to-kite conformation change upon oxidation. The peaks at 262 nm and 374 nm decrease in intensity, presumably as a result of the consumption of **1** by oxidation.

Figure 5 UV-Vis spectrum of **1** in CH_2Cl_2 at different TFA concentrationsFigure 6 Cyclic voltammogram of **1** in CH_2Cl_2 at 0.1 V/s scan rate with TBAPF₆ as supporting electrolyte and Fc/Fc⁺ as external referenceFigure 7 Spectroelectrochemistry of **1** in CH_2Cl_2

To provide further evidence that **1** undergoes a vase-to-kite conformation change upon oxidation, **7**, which constitutes a single quinoxaline wall of **1**, was synthesized (Scheme 2). A low concentration of starting materials was required to produce **7**, presumably at higher concentrations the $\text{S}_\text{N}\text{Ar}$ reaction produces oligomers.



In the absence of the resorcinarene framework, the single cavitand wall **7** should not have the vase-to-kite signatures of the shoulder peak in the UV-Vis spectra. Indeed, the UV-Vis spectra of **7** under different TFA concentrations and spectroelectrochemical studies did not display the shoulder peak below 300 nm (see Supporting Information). As a result, we are confident that this UV-Vis spectroscopic feature is specific to the cavitand and its vase-to-kite conformation change. We observe a new peak at 313 nm, corresponding to the newly formed radical cation of **7**, and a reduction in peak intensities at 264 nm and 363 nm, similar to **1**.

Although UV-Vis spectroscopy provided some evidence for vase-to-kite conformation change upon oxidation, the most definitive evidence is provided by NMR analysis of chemically oxidized cavitand **1**. Nitrosyl tetrafluoroborate (NOBF₄) has been previously reported to oxidize thianthrene, generating the thianthrene radical cation tetrafluoroborate,²² and we treated cavitand **1** with NOBF₄ in deuterated chloroform. However, detecting definitive changes in the methine's chemical shift is potentially complicated by the fact that the oxidized material contains radical cations. Oxidation of the quinoxaline wall **7** showed spectrum wherein the methylene chemical shift was largely unaffected (Figure 8). The observed splitting is presumably due to the two methylene protons having slightly different chemical environments after oxidation. Subjecting cavitand **1** to the same oxidation conditions provided a definitive change in methine chemical shift from 5.20 ppm (vase conformation) to 3.71 ppm (kite conformation) (Figure 9). EPR spectra of both oxidized **1** and **7** showed a single signal with $g_{iso} = 2.0075$ and 2.0076 respectively, suggesting the formation of radical cations from the chemical oxidation. Given that we were able to measure the NMR spectra on this system suggests that the radical cations are sufficiently removed from the methine protons such that they are not dramatically broadened.

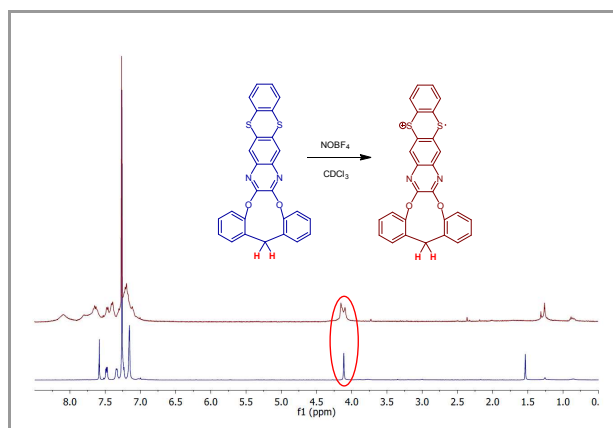


Figure 8 ¹H NMR spectra of **7** before (blue) and after (maroon) oxidation.

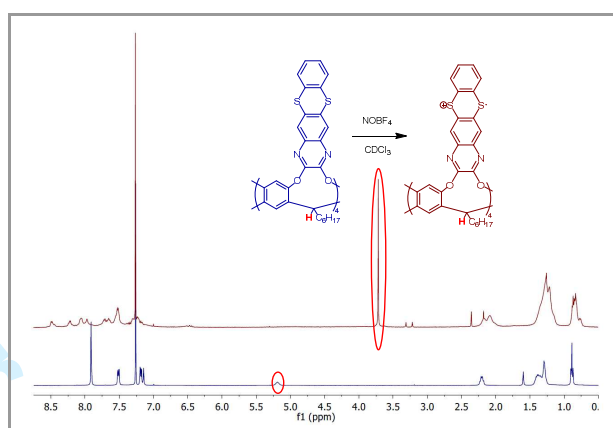


Figure 9 ¹H NMR spectra of **1** before (blue) and after (maroon) oxidation.

In summary, we have successfully demonstrated that cavitand **1** undergoes vase-to-kite conformation change upon oxidation. Thianthrene cavitands represent an attractive scaffold for the formation of new functional supramolecular structures with switchable conformations. Our ongoing studies will focus on generating related functional thianthrene-containing cavitands with applications in electronics and separations.

The experimental section has no title; please leave this line here.

NMR spectra were recorded on a 400 MHz spectrometer. Chemical shifts were reported in ppm and referenced to residual solvent peaks (CDCl₃: δ 7.26 ppm for ¹H, δ 77.16 ppm for ¹³C, DMSO: δ 2.50 ppm for ¹H, δ 39.52 ppm for ¹³C). UV-Vis spectra were obtained using a diode array spectrometer. Electrochemical measurements were carried in a three-electrode cell configuration consisting of a quasi-internal Ag wire reference electrode submerged in 0.01 AgNO₃ / 0.1 M tetrabutylammonium hexafluorophosphate (TBAPF₆) in anhydrous CH₂Cl₂ with TBAPF₆ as supporting electrolyte, a Pt button (1.6 mm in diameter) electrode as the working electrode, and a Pt coil as the counter electrode. The ferrocene/ferrocenium (Fc/Fc⁺) redox couple was used as an external reference. EPR spectra were obtained operating as the X-band with 100 kHz modulation at room temperature. All air and water sensitive synthetic manipulations were performed under an argon atmosphere using standard Schlenk techniques. Anhydrous DMF and 1,2-dichloroethane were purchased from Aldrich as Sure-Seal Bottles and used as received. CH₂Cl₂ and toluene were purified by passage through two alumina columns of an Innovative Technologies purification system. All other chemicals were of reagent grade and used as received.

Procedures

2,3-Dibromothianthrene (2)

To a 3-neck flask containing a solution of triethylamine (0.55 mL) in anhydrous DMF (5 mL), 1,2-benzenedithiol (0.75 mL, 6.53 mmol) in DMF (3 mL) and 1,2-difluoro-4,5-dibromobenzene (1.48 g, 5.44 mmol) in DMF (3 mL) were added *via* different syringes drop by drop at room temperature under argon. The reaction mixture was then stirred overnight at 80 °C. After cooling down to room temperature, the reaction mixture was then concentrated *in vacuo* and added to CH₂Cl₂ (50 mL) and the solution was washed with 1 M HCl solution and water. It was then dried with MgSO₄ and the solvent was removed *in vacuo*. The crude product was further purified by gel column chromatography eluting with hexane/CH₂Cl₂ = 6/1 to yield **2**.

Yield: 1.20 g (59%); white powder; *R_f* = 0.5 (hexane/CH₂Cl₂ = 6/1); mp 159–161 °C.

¹H NMR (400 MHz, CDCl₃) δ: 7.71 (s, 2H), 7.47 (dd, 2H, *J* = 5.8, 3.3 Hz), 7.27 (dd, 2H, *J* = 5.8, 3.3 Hz).

¹³C NMR (100 MHz, CDCl₃) δ: 136.8, 134.7, 132.7, 129.1, 128.3, 123.8.

HRMS (ESI): *m/z* [M]⁺ calcd for C₁₂H₆Br₂S₂: 373.8255; found: 373.8262.

***N,N'*-(Thianthrene-2,3-diyl)bis(1,1-diphenylmethanimine) (3)**

A solution of anhydrous toluene with Pd₂(dba)₃ (0.576 g, 0.629 mmol) and *rac*-BINAP (0.783 g, 1.26 mmol) was degassed by 3 freeze-pump-thaw cycles, filled with argon and stirred at 110 °C for 30 mins. After cooling to room temperature, **2** (2.94 g, 7.86 mmol), NaO^tBu (1.96 g, 20.4 mmol) and diphenylmethanimine (3.45 mL, 20.4 mmol) were added subsequently to the reaction. The reaction was then stirred overnight at 110 °C. The reaction mixture was cooled down and filtered through Celite, washing with CH₂Cl₂. The filtrate was concentrated *in vacuo* and the resulting crude product was purified by gel column chromatography eluting with hexane to ethyl acetate/hexane = 5/95 to obtain **3**.

Yield: 4.02 g (89%); bright yellow foam; *R_f* = 0.2 (ethyl acetate/hexane = 5/95); mp 94–96 °C.

¹H NMR (400 MHz, CDCl₃) δ: 7.64 (d, 4H, *J* = 7.3 Hz), 7.40–7.37 (m, 4H), 7.34–7.29 (m, 6H), 7.24–7.22 (m, 4H), 7.18 (dd, 2H, *J* = 5.6, 3.4 Hz), 6.91 (d, 4H, *J* = 7.2 Hz), 6.64 (s, 2H).

¹³C NMR (100 MHz, CDCl₃) δ: 168.3, 141.6, 139.8, 136.5, 136.2, 130.7, 129.5, 129.3, 129.2, 129.1, 128.6, 128.14, 128.10, 127.4, 121.0.

HRMS (ESI): *m/z* [M+H]⁺ calcd for C₃₈H₂₇N₂S₂: 575.1610; found: 575.1629.

Thianthrene-2,3-diamine (4)

To a solution of **3** (3.97 g, 6.91 mmol) in THF (100 mL) was added 2 M HCl aqueous solution (10.5 mL). The reaction mixture was stirred at room temperature for 30 mins and then concentrated *in vacuo*. To the crude product was added CH₂Cl₂ and the suspension was subjected to sonication for 30 mins, filtered and dried to obtain **4.2HCl**. To a solution of **4.2HCl** in THF (100 mL) was added 2 M NaOH aqueous solution (10 mL). The reaction mixture was stirred at room temperature for 30 mins before concentrating *in vacuo*. To the crude product was added water and the suspension was subjected to sonication for 30 mins, filtered and dried to obtain **4**.

Yield: 1.61 g (95%); off-white powder; mp 222–224 °C.

¹H NMR (400 MHz, DMSO) δ: 7.49 (dd, 2H, *J* = 5.8, 3.3 Hz), 7.26 (dd, 2H, *J* = 5.8, 3.3 Hz), 6.67 (s, 2H), 4.75 (s, 4H).

¹³C NMR (100 MHz, DMSO) δ: 136.7, 135.7, 128.4, 127.4, 120.3, 113.8.

HRMS (ESI): *m/z* [M+H]⁺ calcd for C₁₂H₁₁N₂S₂: 247.0358; found: 247.0354.

Benzo[5,6][1,4]dithiino[2,3-*g*]quinoxaline-2,3-diol (5)

To a solution of **4** (1.59 g, 6.45 mmol) in 4 M HCl aqueous solution (70 mL) was added oxalic acid in 4 M HCl aqueous solution (30 mL). The reaction mixture was stirred under reflux overnight. After cooling to room temperature, the reaction mixture was filtered and the residue was collected and dried to give **5**.

Yield: 1.79 g (92%); light brown powder; mp >300 °C.

¹H NMR (400 MHz, DMSO) δ: 12.00 (s, 2H), 7.59 (dd, 2H, *J* = 5.8, 3.4 Hz), 7.36 (dd, 2H, *J* = 5.8, 3.4 Hz), 7.27 (s, 2H).

¹³C NMR (100 MHz, DMSO) δ: 154.9, 134.6, 128.9, 128.4, 128.3, 126.0, 114.7.

HRMS (DART): *m/z* [M–H]⁺ calcd for C₁₄H₇N₂O₂S₂: 298.9954; found: 298.9934.

2,3-Dichlorobenzo[5,6][1,4]dithiino[2,3-*g*]quinoxaline (6)

To a slurry of **5** (1.79 g, 5.86 mmol) and thionyl chloride (1.3 mL, 17.6 mmol) in anhydrous 1,2-dichloroethane (100 mL) was added 8 drops of anhydrous DMF. The reaction was stirred under reflux overnight. After cooling to room temperature, the reaction mixture was concentrated *in vacuo* and the crude product was purified by gel column chromatography eluting with hexane/toluene = 1/1 to toluene to afford **6**.

Yield: 1.69 g (85%); bright yellow powder; *R_f* = 0.5 (hexane/toluene = 1/1); mp 275–277 °C.

¹H NMR (400 MHz, CDCl₃) δ: 8.09 (s, 2H), 7.53 (dd, 2H, *J* = 5.8, 3.4 Hz), 7.32 (dd, 2H, *J* = 5.8, 3.4 Hz).

¹³C NMR (100 MHz, CDCl₃) δ: 145.9, 140.5, 140.0, 133.8, 129.1, 128.6, 126.3.

HRMS (ESI): *m/z* [M]⁺ calcd for C₁₄H₆Cl₂N₂S₂: 335.9344; found: 335.9355.

Thianthrene-containing cavitand (1)

To a Schlenk flask containing resorcinarene (R = C₆H₁₃)¹¹ (0.167 g, 0.202 mmol) and K₂CO₃ (0.419 g, 3.03 mmol) under argon was added anhydrous DMF (20 mL). After stirring the reaction at room temperature for 20 mins, **6** (0.300 g, 0.890 mmol) was added and the reaction was stirred overnight at 85 °C. After cooling to room temperature, the reaction mixture was poured into 1 M HCl solution. The residue was collected, dissolved in CH₂Cl₂, and filtered to remove an orange residue. The filtrate was collected and concentrated to give the crude product. The crude product was purified by recrystallization (DCM/EtOH) to afford **1**.

Yield: 0.272 g (71%); yellow powder; mp >300 °C.

¹H NMR (400 MHz, CDCl₃) δ: 7.92 (s, 8H), 7.91 (s, 4H), 7.52 (dd, 8H, *J* = 5.8, 3.4 Hz), 7.19 (dd, 8H, *J* = 5.8, 3.4 Hz), 7.14 (s, 4H), 5.20 (s, 4H), 2.20 (dd, 8H, *J* = 14.2, 7.5 Hz), 1.41–1.28 (m, 8H), 0.89 (t, 12H, *J* = 6.8 Hz).

¹³C NMR (100 MHz, CDCl₃) δ: 152.6, 151.9, 139.0, 138.2, 135.1, 134.6, 129.0, 128.1, 126.1, 123.6, 117.9, 35.1, 32.4, 31.9, 29.4, 27.8, 22.8, 14.2.

HRMS (MALDI): *m/z* [M+H]⁺ calcd for C₁₀₈H₉₀N₈O₈S₈: 1884.47; found: 1884.57.

5HBenzo[5,6][1,4]dithiino[2,3-*g*]dibenzo[5,6:8,9][1,4]dioxonino[2,3-*b*]quinoxaline (7)

To a Schlenk flask containing bis(2-hydroxyphenyl)methane (59.3 mg, 0.297 mmol) and K₂CO₃ (164 mg, 1.19 mmol) under argon was added anhydrous DMF (120 mL). The reaction mixture was stirred at room temperature for 20 mins before **6** (100 mg, 0.297 mmol) was added. The reaction was then heated to 85 °C and stirred overnight. After cooling to room temperature, the crude mixture was concentrated *in vacuo* and precipitated into a 1 M HCl solution. The suspension was filtered and the resulting crude solid was purified by recrystallization (CHCl₃/EtOH) to obtain **7**.

Yield: 40 mg (29%); yellow powder; mp >300 °C.

¹H NMR (400 MHz, CDCl₃) δ: 7.58 (s, 2H), 7.48 (dd, 8H, *J* = 5.8, 3.4 Hz), 7.35–7.33 (m, 2H), 7.25 (dd, 2H, *J* = 5.8, 3.4 Hz), 7.17–7.15 (m, 6H), 4.11 (s, 2H).

¹³C NMR (100 MHz, CDCl₃) δ: 150.9, 148.9, 136.9, 135.3, 134.9, 132.0, 131.2, 129.0, 128.0, 127.4, 125.8, 125.5, 121.6, 30.0.

HRMS (DART): *m/z* [M+H]⁺ calcd for C₂₇H₁₇N₂O₂S₂: 465.0726; found: 465.0711.

Acknowledgment

This work was supported by the National Science Foundation (NSF) Center for Energy Efficient Electronics Science (E3S) (Award ECCS-0939514). W.J.O. acknowledges the support of Agency for Science, Technology and Research (A*STAR), Singapore for a graduate scholarship. F.B. thanks FIRB RINAME (RBAP114AMK) for financial support.

Supporting Information

YES

Primary Data

NO

References

- (1) New address: F. Bertani, School of Chemistry, University of Tokyo, Department of Applied Chemistry, Japan.
- (2) Moran, J. R.; Karbach, S.; Cram, D. J. *J. Am. Chem. Soc.* **1982**, *104*, 5826.
- (3) Azov, V. A.; Beeby, A.; Cacciarini, M.; Cheetham, A. G.; Diederich, F.; Frei, M.; Gimzewski, J. K.; Gramlich, V.; Hecht, B.; Jaun, B.; Lатыchevskaya, T.; Lieb, A.; Lill, Y.; Marotti, F.; Schlegel, A.; Schlittler, R. R.; Skinner, P. J.; Seiler, P.; Yamakoshi, Y. *Adv. Funct. Mater.* **2006**, *16*, 147.
- (4) (a) Bertani, F.; Riboni, N.; Bianchi, F.; Brancatelli, G.; Sterner, E. S.; Pinalli, R.; Geremia, S.; Swager, T. M.; Dalcanele, E. *Chem. Eur. J.* **2016**, *22*, 3312. (b) Pinalli, R.; Brancatelli, G.; Pedrini, A.; Menozzi, D.; Hernández, D.; Ballester, P.; Geremia, S.; Dalcanele, E. *J. Am. Chem. Soc.* **2016**, *138*, 8569.
- (5) (a) Zampolli, S.; Elmi, I.; Mancarella, F.; Betti, P.; Dalcanele, E.; Cardinali, G. C.; Severi, M. *Sens. Actuators B* **2009**, *141*, 322. (b) Pinalli, R.; Dalcanele, E. *Acc. Chem. Res.* **2013**, *46*, 399.
- (6) (a) Purse, B. W.; Rebek, J. *Proc. Natl. Acad. Sci. USA* **2005**, *102*, 10777. (b) Hooley, R. J.; Rebek Jr, J. *Chem. Biol.* **2009**, *16*, 255.
- (7) (a) Rebek, J. *Acc. Chem. Res.* **2009**, *42*, 1660. (b) Dumele, O.; Trapp, N.; Diederich, F. *Angew. Chem. Int. Ed.* **2015**, *54*, 3290.
- (8) Pochorovski, I.; Diederich, F. *Acc. Chem. Res.* **2014**, *47*, 2096.
- (9) (a) Bianchi, F.; Bedini, A.; Riboni, N.; Pinalli, R.; Gregori, A.; Sidisky, L.; Dalcanele, E.; Careri, M. *Anal. Chem.* **2014**, *86*, 10646. (b) Riboni, N.; Trzcinski, J. W.; Bianchi, F.; Massera, C.; Pinalli, R.; Sidisky, L.; Dalcanele, E.; Careri, M. *Anal. Chim. Acta* **2016**, *905*, 79.
- (10) Moran, J. R.; Ericson, J. L.; Dalcanele, E.; Bryant, J. A.; Knobler, C. B.; Cram, D. J. *J. Am. Chem. Soc.* **1991**, *113*, 5707.
- (11) Skinner, P. J.; Cheetham, A. G.; Beeby, A.; Gramlich, V.; Diederich, F. *Helv. Chim. Acta* **2001**, *84*, 2146.
- (12) Frei, M.; Marotti, F.; Diederich, F. *Chem. Commun.* **2004**, 1362.
- (13) Frei, M.; Diederich, F.; Tremont, R.; Rodriguez, T.; Echegoyen, L. *Helv. Chim. Acta* **2006**, *89*, 2040.
- (14) (a) Pochorovski, I.; Boudon, C.; Gisselbrecht, J.-P.; Ebert, M.-O.; Schweizer, W. B.; Diederich, F. *Angew. Chem. Int. Ed.* **2012**, *51*, 262. (b) Pochorovski, I.; Ebert, M.-O.; Gisselbrecht, J.-P.; Boudon, C.; Schweizer, W. B.; Diederich, F. *J. Am. Chem. Soc.* **2012**, *134*, 14702. (c) Pochorovski, I.; Milić, J.; Kolarski, D.; Gropp, C.; Schweizer, W. B.; Diederich, F. *J. Am. Chem. Soc.* **2014**, *136*, 3852.
- (15) Ruiz-Botella, S.; Vidossich, P.; Ujaque, G.; Vicent, C.; Peris, E. *Chem. Eur. J.* **2015**, *21*, 10558.
- (16) (a) Shine, H. J.; Piette, L. *J. Am. Chem. Soc.* **1962**, *84*, 4798. (b) Rapta, P.; Kress, L.; Hapiot, P.; Dunsch, L. *Phys. Chem. Chem. Phys.* **2002**, *4*, 4181.
- (17) Kim, S.; Kwon, Y.; Lee, J.-P.; Choi, S.-Y.; Choo, J. *J. Mol. Struct.* **2003**, *655*, 451.
- (18) Bock, H.; Rauschenbach, A.; Näther, C.; Kleine, M.; Havlas, Z. *Chem. Ber.* **1994**, *127*, 2043.
- (19) Yu, H.-h., Massachusetts Institute of Technology, 2003.
- (20) Rabbani, M. G.; Reich, T. E.; Kassab, R. M.; Jackson, K. T.; El-Kaderi, H. M. *Chem. Commun.* **2012**, *48*, 1141.
- (21) Azov, V. A.; Jaun, B.; Diederich, F. *Helv. Chim. Acta* **2004**, *87*, 449.
- (22) Boduszek, B.; Shine, H. J. *J. Org. Chem.* **1988**, *53*, 51

Redox Switchable Thianthrene Cavitands

Wen Jie Ong,^a Federico Bertani,^b Enrico Dalcanale,^b Timothy M. Swager^{a,*}

^aDepartment of Chemistry, Massachusetts Institute of Technology, 77 Massachusetts Avenue, Cambridge, Massachusetts 02139, United States

^bDepartment of Chemistry, University of Parma and INSTM RU, Parco Area delle Scienze 17/A, Parma 43124, Italy

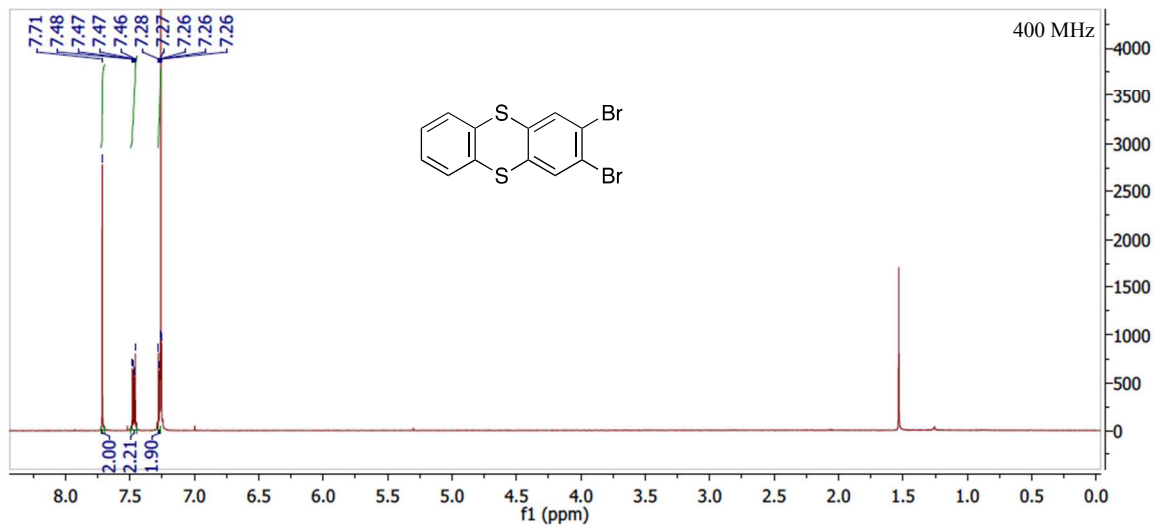
E-mail: tswager@mit.edu

Supporting Information

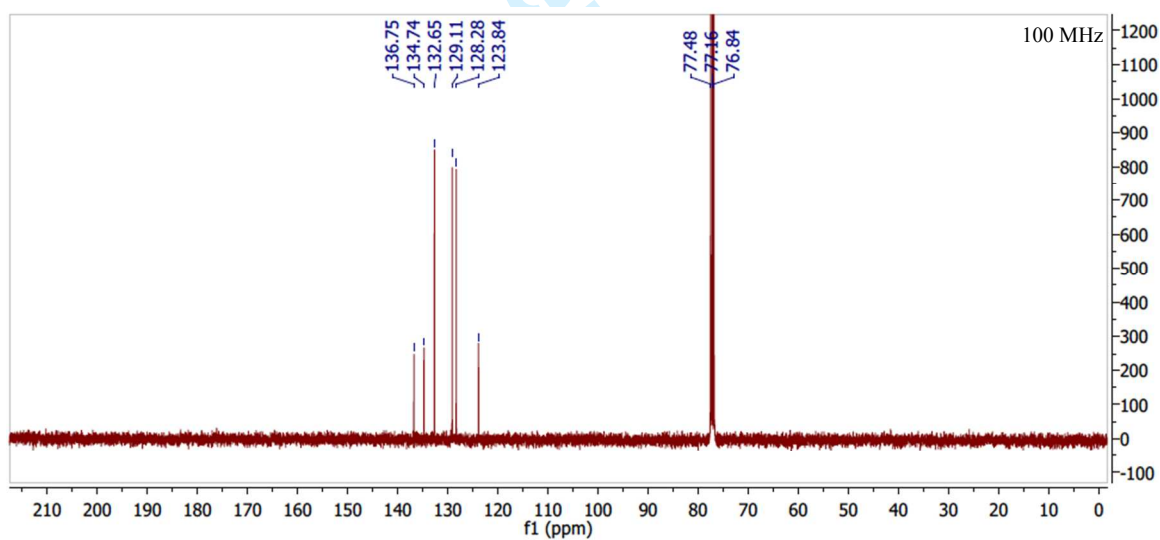
List of Contents

¹ H and ¹³ C NMRs of Compounds	2
Plot of temperature against methine chemical shift of 1	9
UV-Vis spectrum of 7 at different TFA concentrations.....	10
Spectroelectrochemistry of 7	11
EPRs of Chemically Oxidized 1 and 7	12

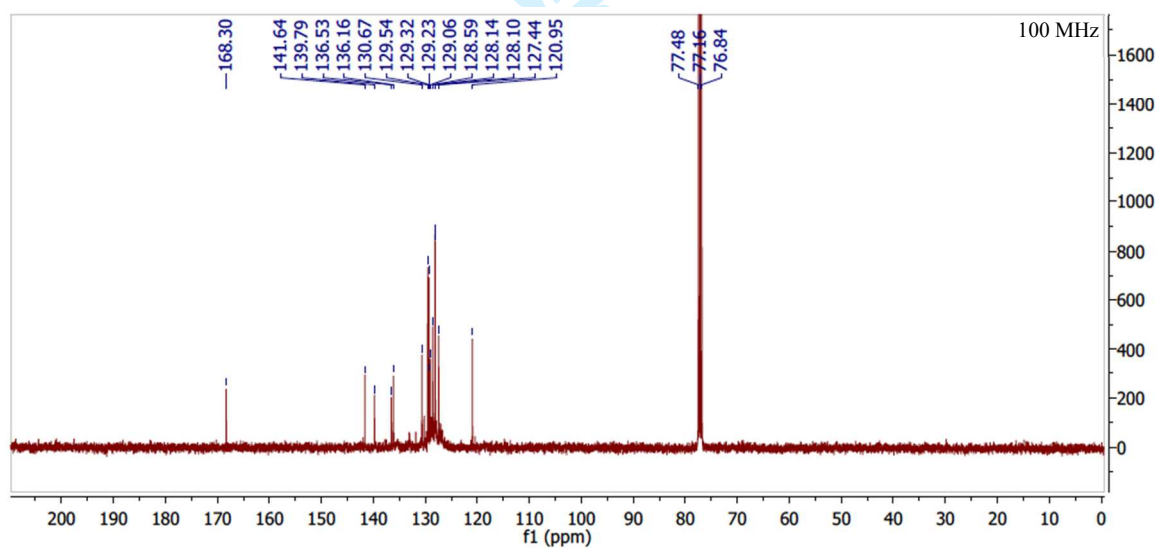
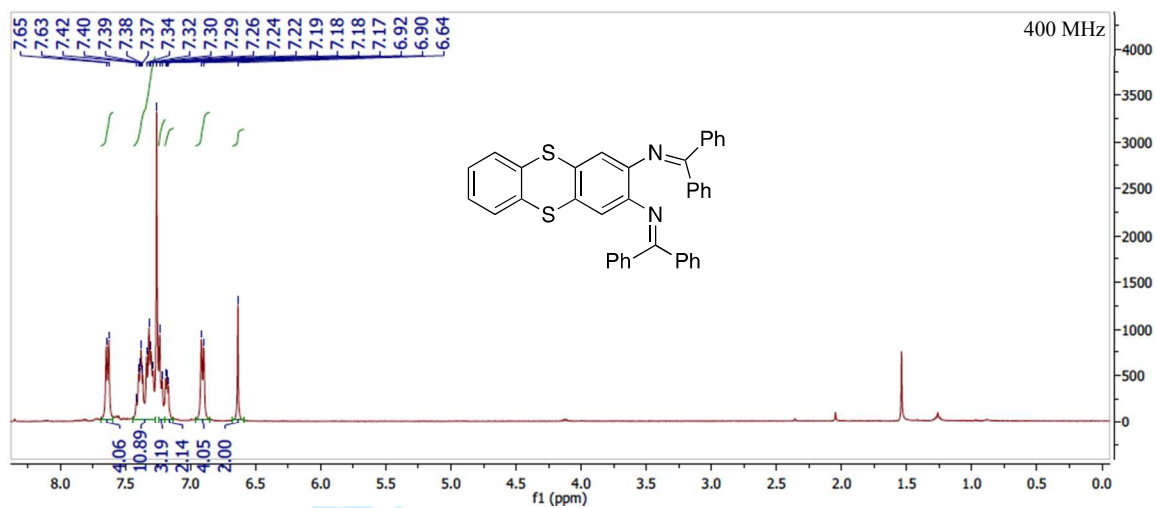
^1H NMR of **2** in CDCl_3



^{13}C NMR of **2** in CDCl_3

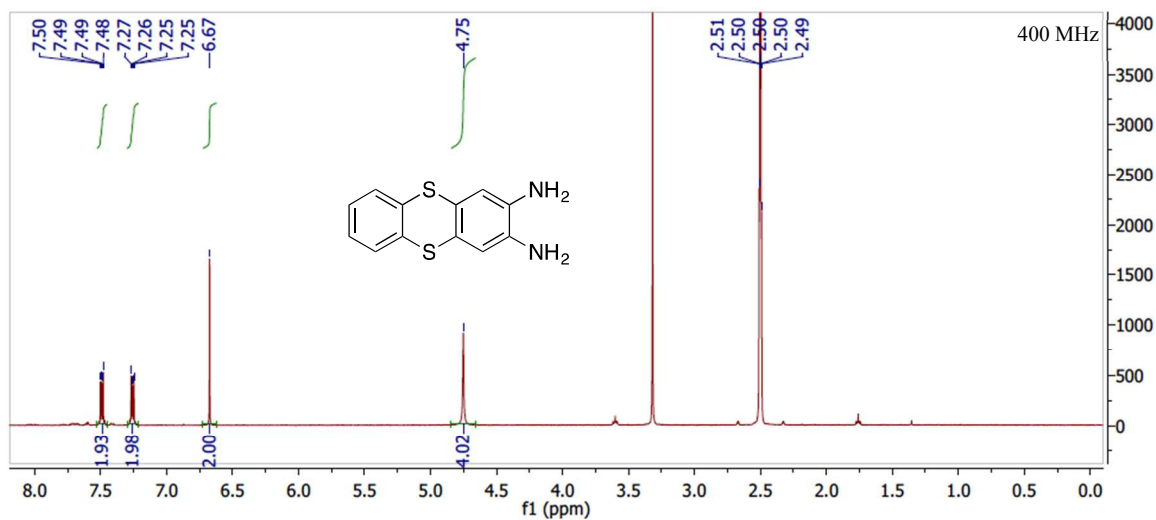


^1H NMR of **3** in CDCl_3

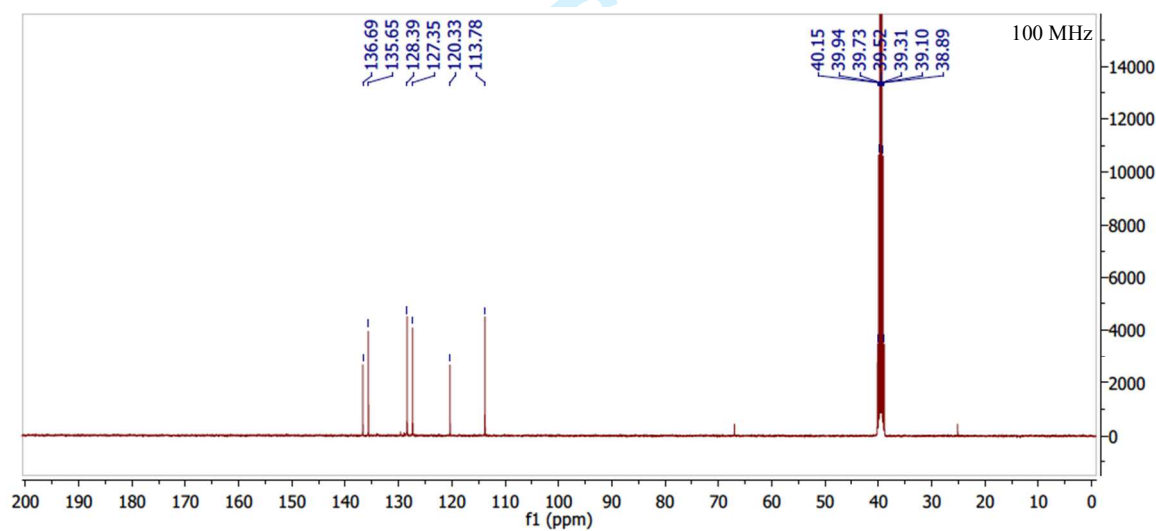


^{13}C NMR of **3** in CDCl_3

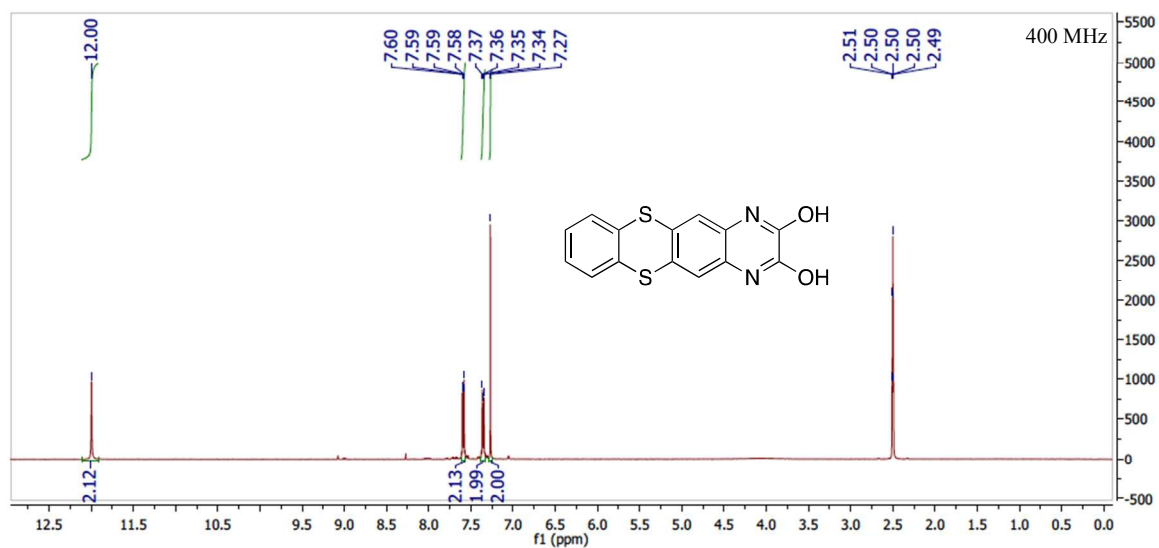
^1H NMR of **4** in DMSO-d_6



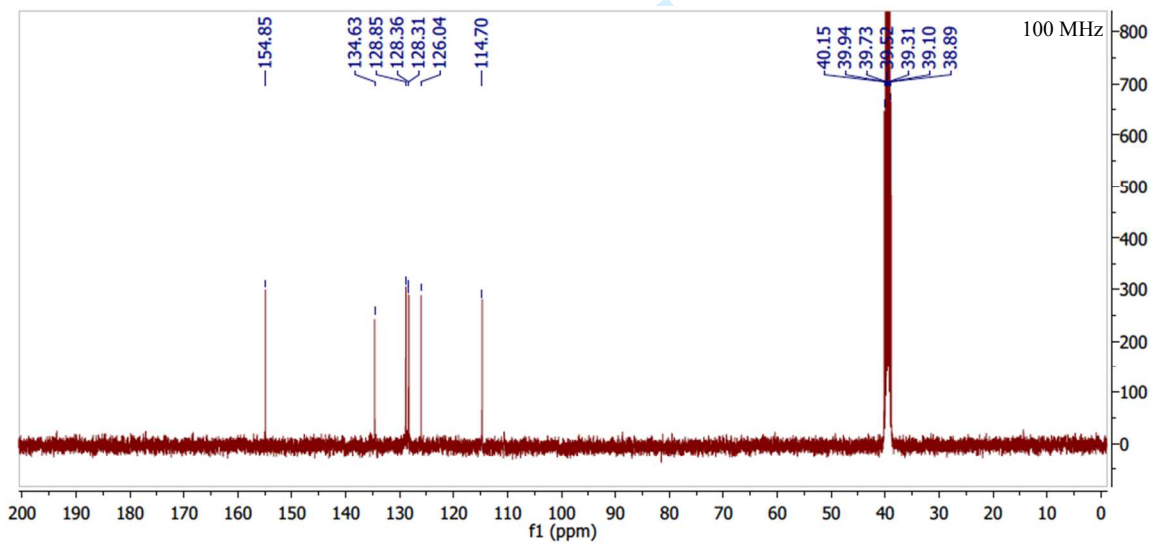
^{13}C NMR of **4** in DMSO-d_6



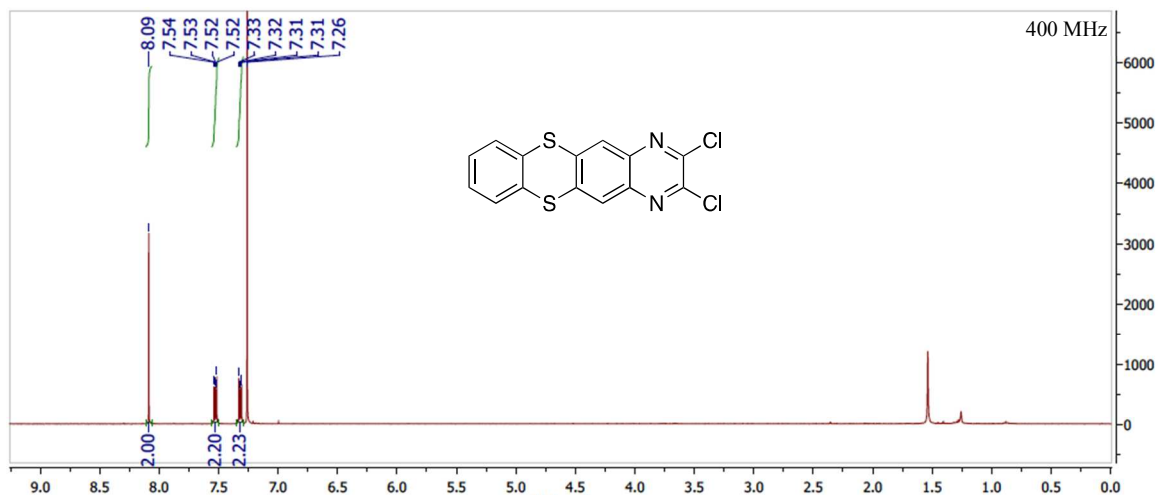
^1H NMR of **5** in DMSO-d_6



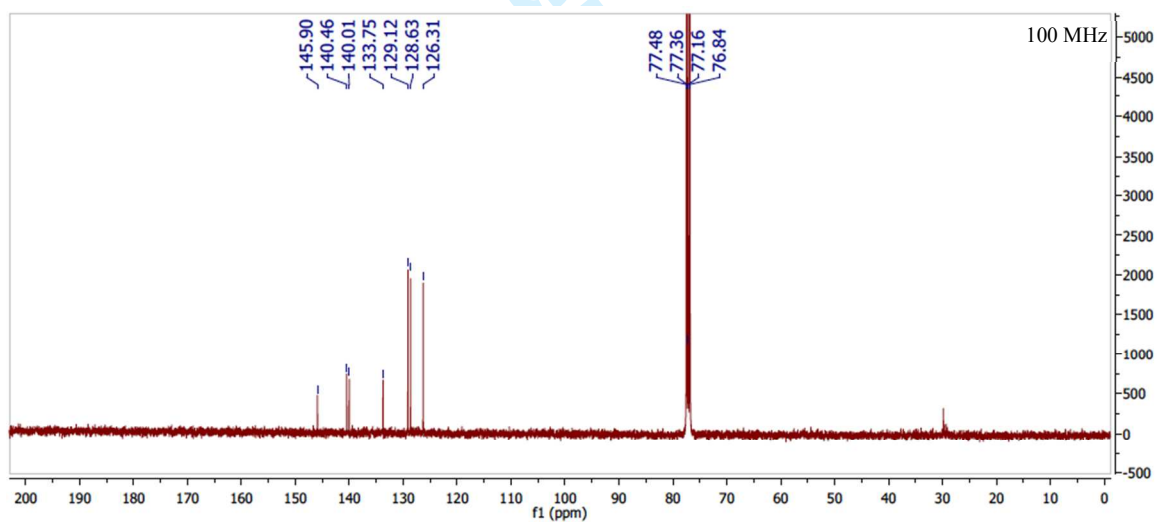
^{13}C NMR of **5** in DMSO-d_6



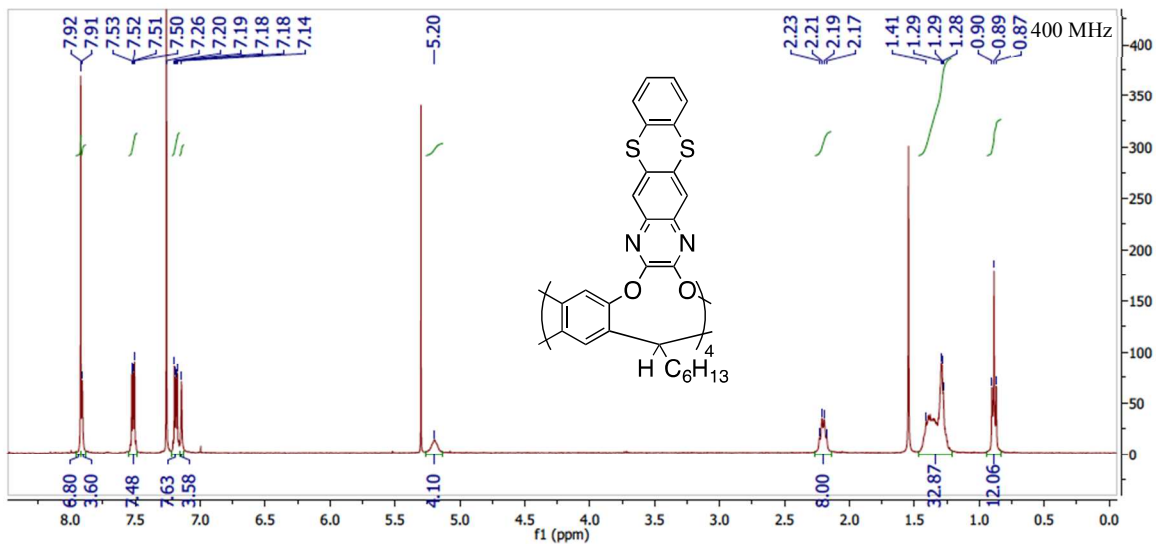
^1H NMR of **6** in CDCl_3



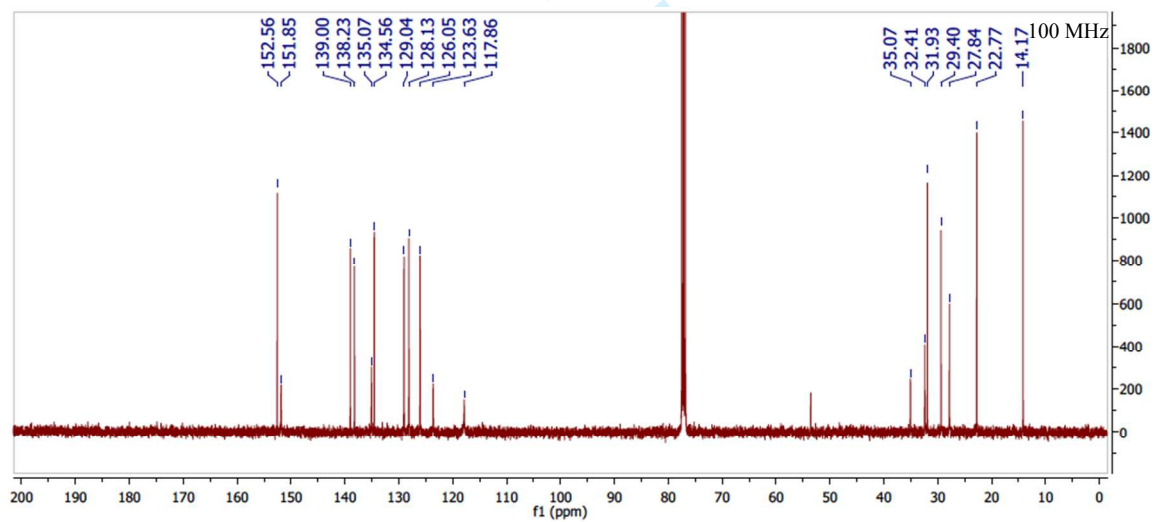
^{13}C NMR of **6** in CDCl_3



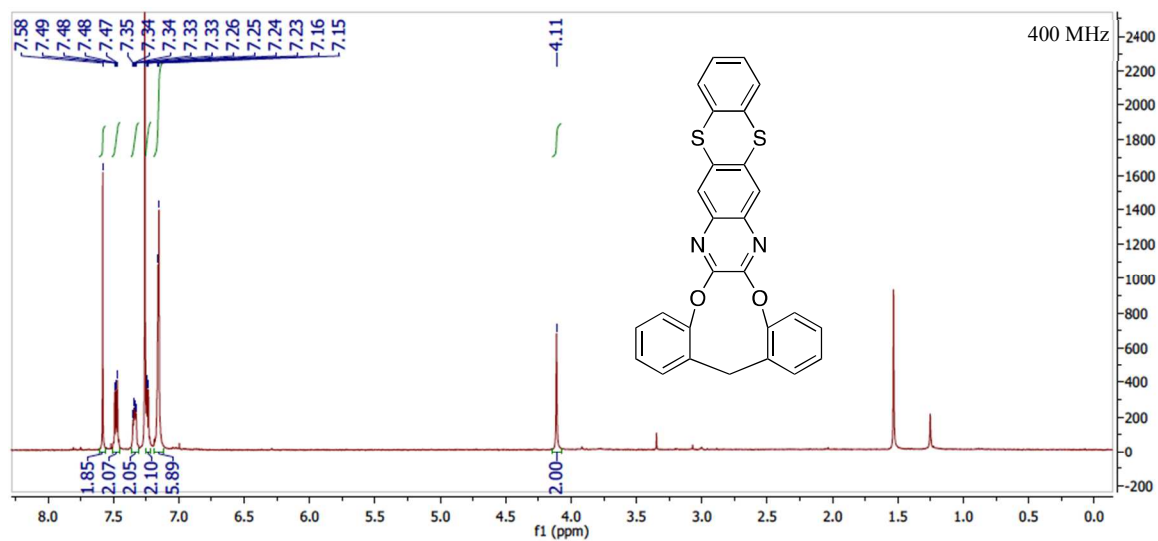
^1H NMR of **1** in CDCl_3



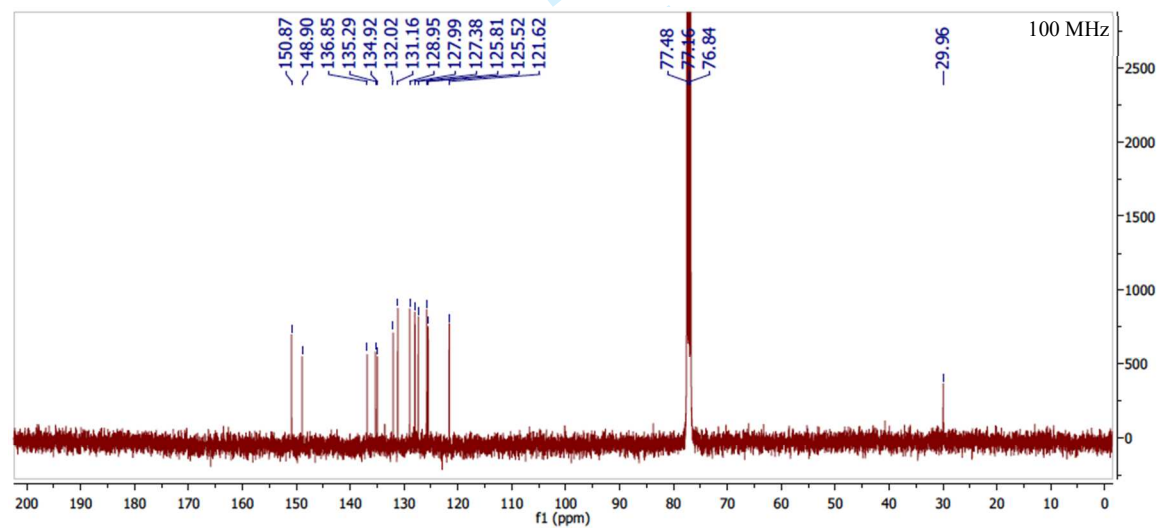
^{13}C NMR of **1** in CDCl_3



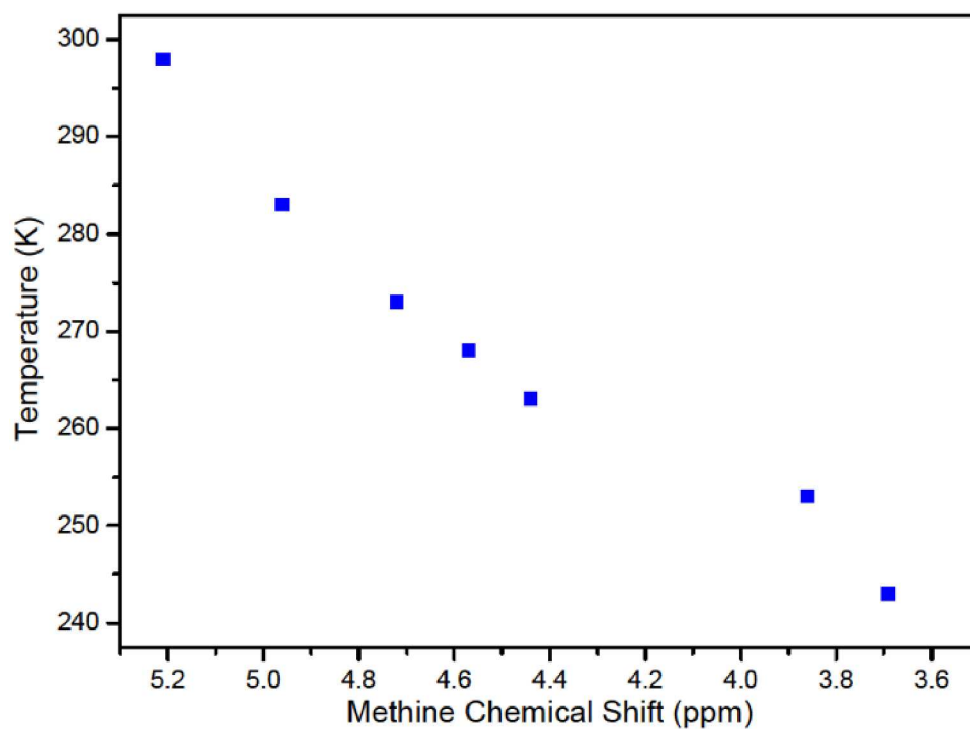
^1H NMR of **7** in CDCl_3



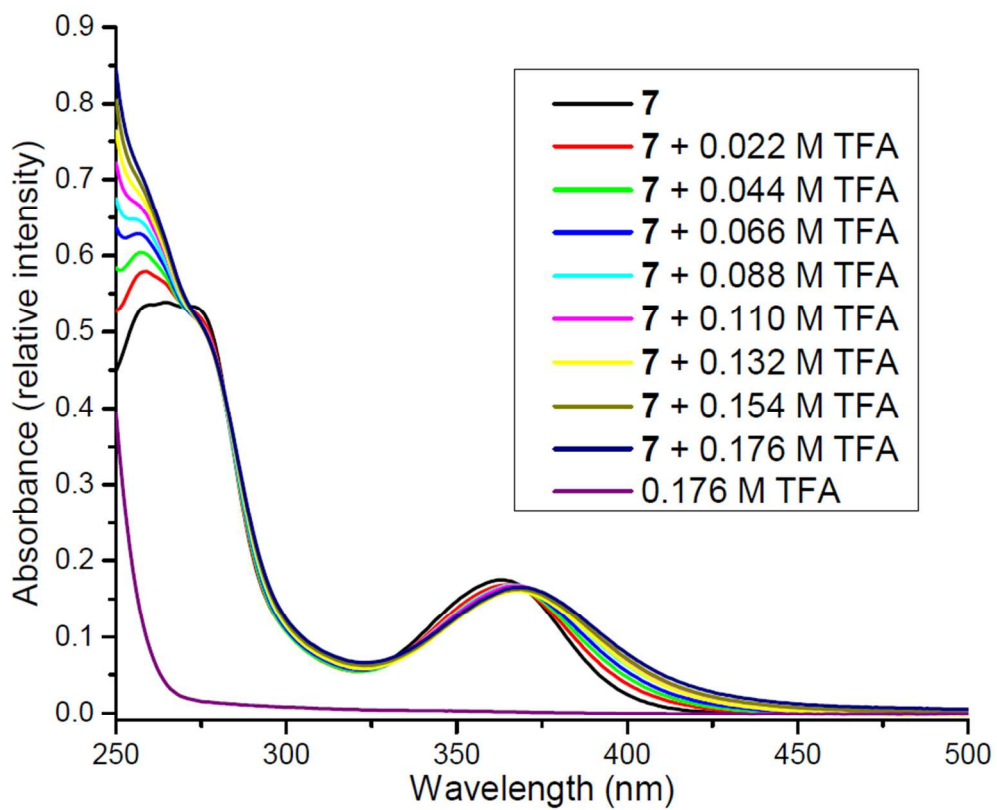
^{13}C NMR of **7** in CDCl_3



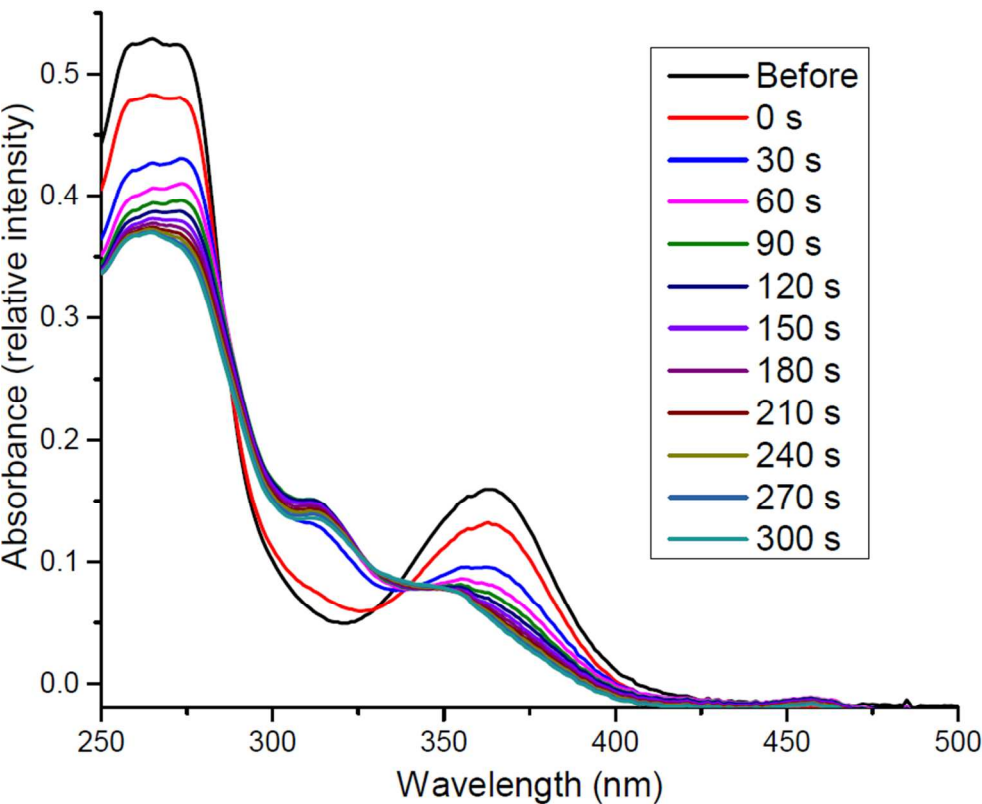
Plot of temperature against methine chemical shift of **1** in CDCl_3

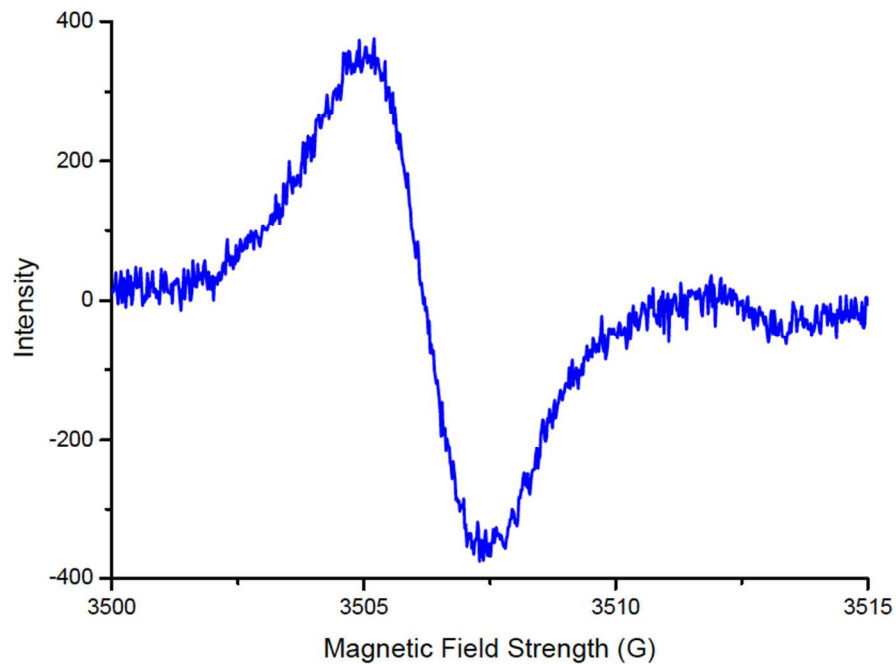


UV-Vis spectrum of **7** in CH₂Cl₂ at different TFA concentrations



Spectroelectrochemistry of **7** in CH₂Cl₂



EPR of Chemically Oxidized **1**EPR of Chemically Oxidized **7**